DEMONSTRATION OF MODEL-BASED CONTROL OF THERMOPLASTIC CONTINUOUS RESISTANCE WELDING

Barroeta Robles, J., Palardy-Sim, M., Stanczak, J., Roy, S., Ferland, F., Elame, H. R. J., Laurin, H., Octeau, M-A., and Yousefpour, A.
National Research Council Canada, Montréal, Canada
* Corresponding author (**Julieta.BarroetaRobles@nrc-cnrc.gc.ca**)

Atkinson, S., Vaziri, R., and Poursartip, A.
Composites Research Network, Department of Materials Engineering, The University of British Columbia, Vancouver, Canada

Endrass, M., Larsen, L., and Kupke, M.
Center for Lightweight Production Technology, Augsburg, Germany

Keywords: *Thermoplastic, resistance welding, process modelling*

ABSTRACT

Integrated design can extend the lightweighting potential of structural composite components in the aerospace industry. However, with increased component complexity and size, aspects such as manufacturing complexity and costs predominate, which is why differential construction is still the state of the art today. Welding technologies, such as resistance welding, provide an approach for producing integrated fibre-reinforced high-performance thermoplastics structures. This publication highlights the current development work in the field of continuous resistance welding. This process uses Joule heating of a conductive insert to generate heat, locally melting the joint along the mating surfaces of the two consolidated components to be joined. In the present application, continuous resistance welding (CRW) relies on discretizing the application of current to the continuous electrical insert, welding locally under a mobile end effector. A model based on fundamental physics encompassing both electrical and thermal phenomena was developed and used finite element to simulate weld interface temperature based on initial setup parameters and characterized properties. A surrogate model was used to predict weld interface temperatures and a control scheme based on this prediction was used to demonstrate CRW on a robotic platform.

1 Introduction

Thermoplastic composites (TPCs) are seeing an increased usage in aerospace applications [1]. These materials have the ability to be melted multiple times, thus enabling joining methods such as welding, as an alternative to mechanical fastening and adhesive bonding. Thermoplastic welding provides a clear advantage with new pathways to robust, industrial assemblies of complex components and sub-assemblies [2]. For instance, static resistance welding has already been demonstrated to join clips and brackets, and full-scale structures such as the TPC rear pressure bulkhead with welds of approximately 1.5 m long [3, 4]. To fulfill the structural integration requirements of large TPC structures, static resistance welding is no longer suitable. Geometrical limitations, increased power, and pressure requirements make the process unfeasible. Continuous resistance welding (CRW) is introduced as a solution and a way to fulfill these requirements. In the CRW process, a mobile end effector moves along the weld substrate applying consolidation pressure (to ensure intimate contact during the melt and cooling phases) and locally heats the interface via the Joule effect in order to melt the polymer. To reduce the required input power, the electrodes are discrete while a heating element made out of stainless-steel mesh or carbon fibre prepreg is continuous. To address automation related aspects, the end effector can be mounted onto an industrial robot to allow continuous welding of large and complex structures.

During the welding process, there will be variations within a part (e.g. varying contact between electrode and mesh, causing varying current distribution) which makes real-time process control critical. Thus, using fundamental physics encompassing both electrical and thermal phenomena, a finite element (FE) model was developed and used to predict the temperature distribution at the weld interface based on initial setup parameters and active process feedback (e.g.: power supply current feedback, and thermocouples). These models have been validated and the data has been published previously [5, 6]. The objective of this paper is to demonstrate real time model-based control of the CRW process, combining process modelling and automation expertise to shorten the technology development time. The experimental setup, methodology, and scale-up to the integration of the CRW test bench onto an industrial robot are presented. This work was performed as part of a collaboration between the National Research Council Canada (NRC), The University of British Columbia (UBC), and the German Aerospace Centre (DLR) and is a follow-up to a paper presented at CANCOM 2022 [7].

2 Experimental Setup

The CRW system used in this work consists of a welding end effector, pressure pad, and substrate support, as illustrated in Figure 1. The welding end effector moves along the weld line of the specimens. A current is passed through a pair of copper rollers which contact a series of adjacent discrete copper blocks as the welding end effector is in motion. A continuous heating element placed at the weld interface is contacted by the discrete copper blocks. A compaction shoe applies consolidation pressure through a series of parallel rollers to ensure full consolidation during the weld.

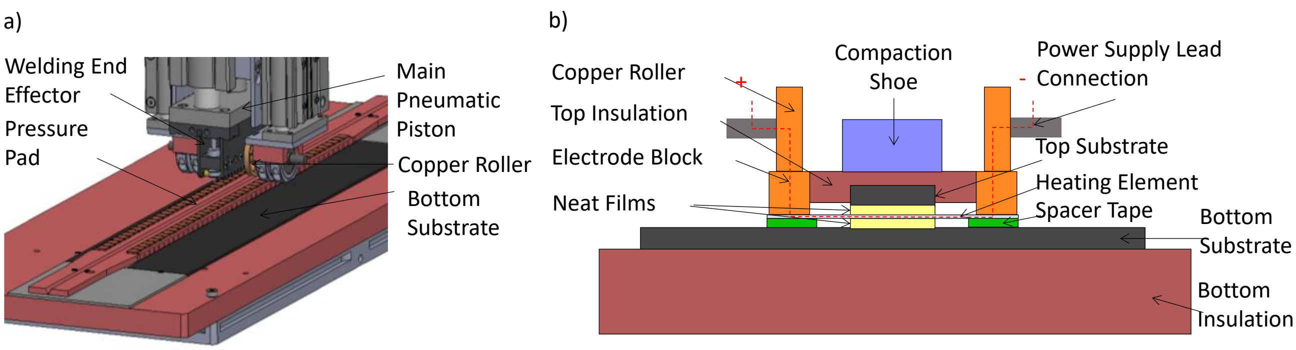

Figure 1. Isometric view of the Continuous Resistance Welding (CRW) benchtop system (left) and simplified cross-section of the CRW setup (right)

Extensive modeling work was performed in order to simulate the process and documented by Atkinson [5, 8]. These simulations used a systems definition previously presented in [5] to determine the power and speed inputs that were required to obtain a high-quality weld. These simulations were able to predict the temperature at the weld interface and provide the sensitivity of different parameters. The results showed that predicted temperatures were far more sensitive to variations in electrical properties (e.g., characterized contact resistance) than other physical properties of the system. Since the computational time of the FE model was found to be long for closed-loop process control, a surrogate model was used to predict process feedback based on previously generated FE model results. The surrogate model used real time process outputs (e.g.: current and time) to predict temperature along the center of the weld line. A control scheme using the predictions of the surrogate model to adjust speed of the mobile end effector was developed to ensure the process temperature targets were met. The first step included validation of these models, which was conducted using the benchtop CRW system (Figure 1) with 16-ply, $[0/90]_{4s}$ glass fibre (GF) poly-ether-ether-ketone (PEEK) laminates. The heating element was stainless steel (SS) 304 plain weave metal mesh which has previously demonstrated to produce high-quality welds [9]. The benchtop CRW system was then integrated onto a Kuka industrial robot at DLR (Figure 2) for demonstration of the technology in an industrial setting, addressing questions related to communication of the robot with the end-effector and positional accuracy.

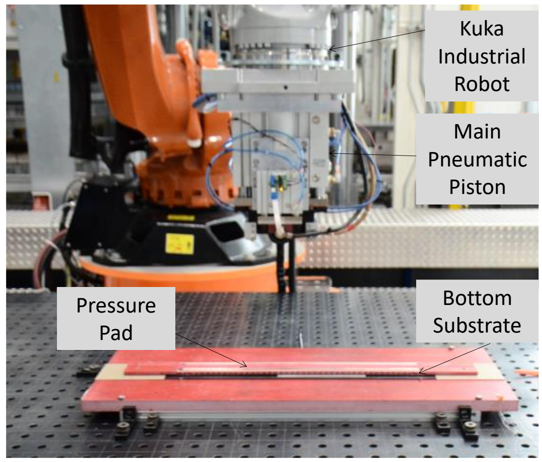

Figure 2. Integration of welding end-effector onto industrial Kuka robot

To demonstrate the control scheme, 16-ply carbon fibre (CF) PEEK laminates with a layup of $[45/-45/0/90]_{2s}$ were used with the SS mesh as the heating element and with two 0.127 mm neat PEEK resin film layers. Preliminary welding trials were performed to ensure current leakage was not present during the process. To evaluate the model's ability to control the process, a disturbance was introduced in the process in the form of an aluminum heat sink that was inserted within the insulating tooling material. Preliminary simulations showed this aluminum insert would cause a difference of ~50°C at the weld interface at the location of the aluminum block, as shown in Figure 3.

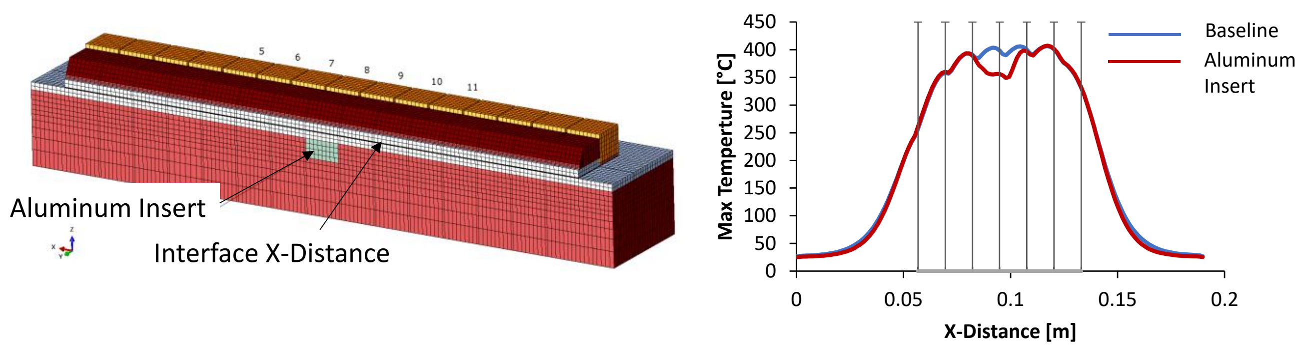

Figure 3: Effect of aluminum heat sink when placed within the insulation board

The FE model was used to provide recommendations to adjust key process parameters (e.g.: speed) to ensure that the temperature at the interface would reach the target processing window. For this welding process and material, this window was defined to be above 343 °C (i.e., above the melting temperature of PEEK) and below 450 °C (i.e., to prevent degradation of PEEK) [9]. The defined processing envelope is shown in Figure 4 a) and b), highlighted by the green region. Figure 4 a) shows that when the heat sink was present within the insulating tooling (highlighted by the blue region in the figure), it was not possible to reach the desired processing temperature if speed was kept at a constant value (1.2 mm/s). Figure 4 b) shows that if the speed of the welding end effector was reduced from 1.2 mm/s to 1 mm/s when passing over the region where the heat sink was present, it was possible to stay within the desired processing window throughout the weld.

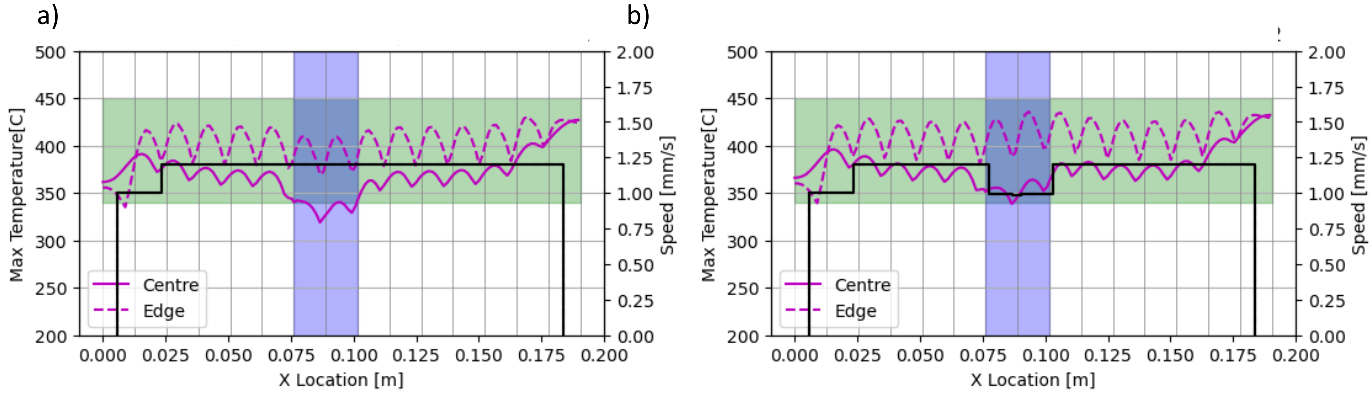

Figure 4: Welding temperature at the interface when passing over an aluminum heat sink without (a) and with (b) speed adjustment as recommended by the model

For the demonstration of the technology, welds were performed with regions representing four tests cases, as follows:

1. Constant speed (based on FE model) without an aluminum heat sink
2. Constant speed (based on FE model) with an aluminum heat sink and active control via the surrogate model
3. Emergency stop case (i.e., to emulate an operator using an emergency stop and restarting shortly after)
4. Edge effects (start and end of the weld)

3 Results

To first validate that current leakage was not present when using CF/PEEK specimens, welds were performed aiming to stay below and above the melting temperature of PEEK (343 °C). Welds were thus performed at 5 V and 6 V as shown in Figure 5 a), and b), respectively. The current response of the 5 V and 6 V cases were similar to the matching tests performed using glass fibre and reported previously in [6]. Thus, significant current leakage was not present during the tests performed with CF reinforced laminates, likely due to the preferential laminate stacking sequence.

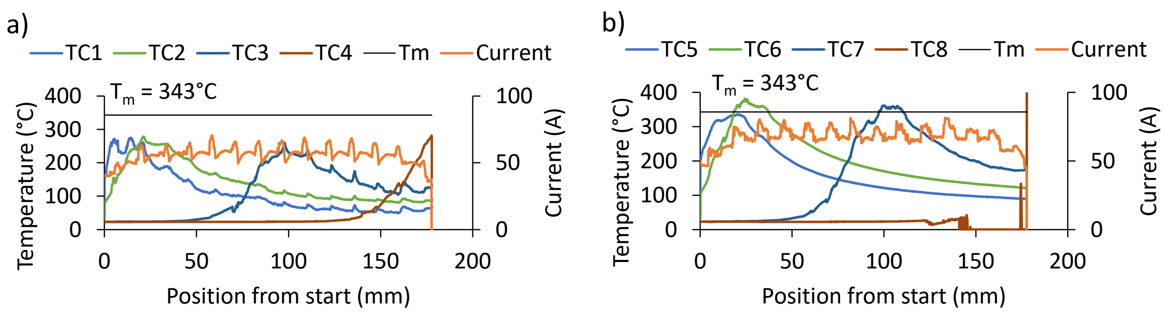

Figure 5: Weld performed at 5 V (left) and 6 V (right) to stay below and above the melting temperature of PEEK

These results provided the confidence required to use the CF/PEEK laminates for the demonstration. Four K-type thermocouples were placed at the interface in key locations to demonstrate the ability of the model-based control scheme to adjust the current and speed setpoints during the four aforementioned cases in Section 2 and maintain a constant weldline temperature.

The FE model was used to identify nominal parameters (current and end effector speed targets) for a successful weld based on nominal and previously characterized values. When process deviations were encountered (i.e., aluminum heat sink), the surrogate model control scheme provided real-time adjustments and temperature prediction based on process feedback. These process deviations from target were used in the real-time evaluation of weld temperature at the centre and the edge to adjust speed. The resulting predictions of the surrogate model and the thermocouple measurements are shown in Figure 6 for the demonstration case. Overall, these results showed that the surrogate model was able to match the thermocouple measurements closely, and thus provided the required adjustments to the input power and speed.

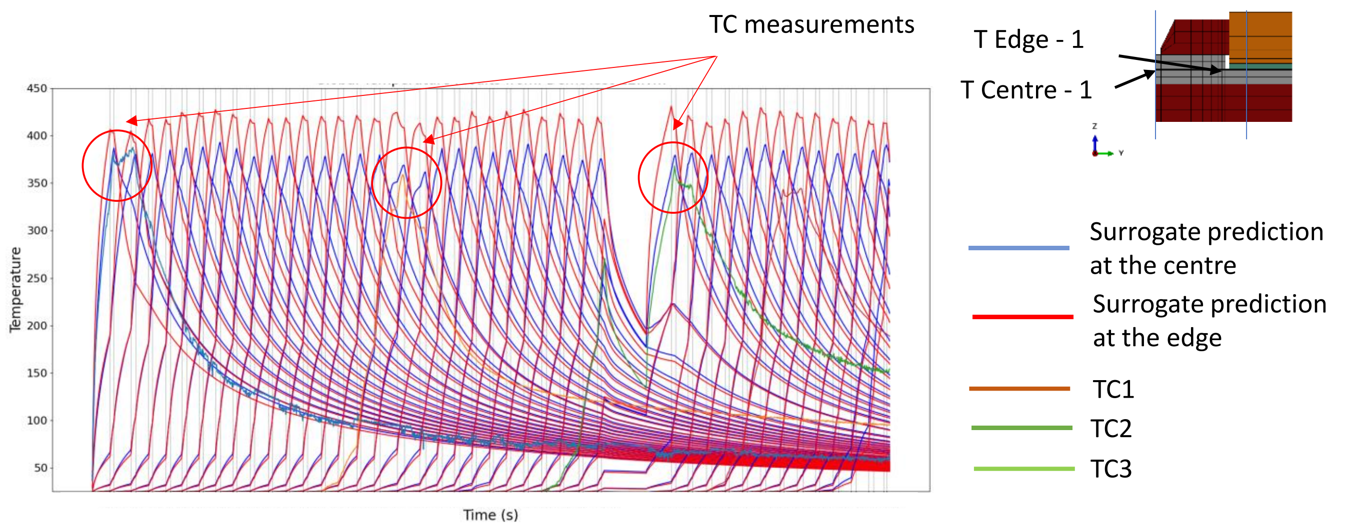

Figure 6: Surrogate model predictions and thermocouple measurements at key locations along the welding interface

To evaluate weld quality, ultrasonic C-scan inspection was conducted using an OLYMPUS OmniScan® SX phased array flaw detector with a 5L64-NW1 probe, and a SNW1-OL-IHC wedge mounted on a 2-axis encoding GLIDER X-Y. The results are shown in Figure 7. The regions highlighted in red were indicative of attaining a full weld, whereas the regions highlighted by the arrows (highlighted in blue) showed zones of incomplete melt and poor consolidation. These regions matched the location of the thermocouples, which were insulated using Kapton polyimide tape, thus explaining some of the disturbances observed in the scans. The scans showed full melt and consolidation at the start and end conditions, and at the aluminum block, thus demonstrating the capacity of model-based control.

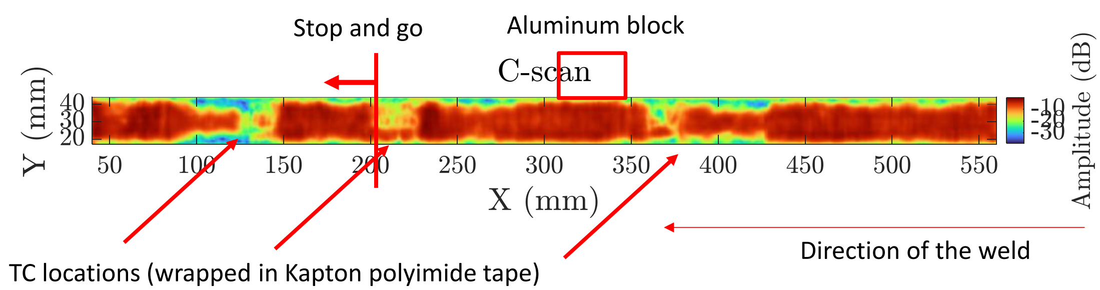

Figure 7: Ultrasonic inspection to investigate the quality of the welded joint

4 Conclusions

FE modelling based on fundamental physics was developed and validated using a CRW test bench. A CRW welding end-effector was integrated onto a Kuka industrial robot to demonstrate model-based control of the welding process. A surrogate model and control scheme were developed to use simulation outputs and real time process feedback to predict temperature along the weld line and actively control the process. C-scans were performed to evaluate weld quality, indicating characteristic signs of a good quality weld throughout most of the specimen.

5 Acknowledgements

The authors of this paper would like to Jim Pratt, Kevin Dupuis and Innocente Fabbro from Syensqo for their support for this project.

6 References

[1] D. Mathijsen, "Leading the way in thermoplastic composites," *Reinforced Plastics,* vol. 60, no. 6, 2016.

[2] A. Yousefpour, M. Hojjati and J.-P. Immarigeon, "Fusion bonding/welding of thermoplastic composites," *Journal of Thermoplastic Composite Materials,* vol. 17, no. 4, pp. 303-341, 2004.

[3] DLR, "Aviation - New technology for the manufacture of CFRP components," 25 April 2018. [Online]. Available: https://www.dlr.de/en/latest/news/2018/2/20180425_aviation-new-technology-for-the-manufacture-of-cfrp-components_26940. [Accessed 15 May 2024].

[4] S. L. Veldman, P. Kortbeek, P. C. Wolcken, R. Herrmann, J. Kos and a. I. V. Fernandez, "Development of a multifunctional fuselage demonstrator," in *Aerospace Europe Conference*, Bordeaux, 2020.

[5] S. Atkinson, S. Nesbitt, R. Vaziri and A. Poursartip, "A Process Simulation Framework for In-Line Control of Continuous Resistance Welding," in *SAMPE*, Seattle, 2023.

[6] M. Palardy-Sim, J. Barroeta Robles, M.-A. Octeau, S. Roy and A. Yousefpour, "Towards in-line control of continuous resistance welding for joining structural thermoplastic composites," *SAMPE Journal: Thermoplastics Edition,* vol. 59, no. 5, pp. 9-17, 2023.

[7] M. Palardy-Sim, J. Barroeta Robles, M.-A. Octeau, S. Roy, A. Guthrie, F. Ferland and A. and Yousefpour, "Towards robust, non-application specific continuous resistance welding," in *Canadian International Conference on Composite Materials*, Fredericton, Moncton, NB, 2022.

[8] S. Atkinson, "A process simulation framework for continuous resistance welding of thermoplastic composites," Vancouver, 2024.

[9] E. Talbot, P. Hubert, M. Dubé and A. Yousefpour, "Optimization of thermoplastic composites resistance welding parameters based on transient heat transfer finite element model," *Journal of Thermoplastic Composite Material,* vol. 26, no. 5, pp. 699-717, 2011.